

Collective excitations of ^{194}Pt in low energy neutron scattering

M. C. Mirzaa,* J. P. Delaroche,† J. L. Weil, J. Hanly, and M. T. McEllistrem
Department of Physics and Astronomy, University of Kentucky, Lexington, Kentucky 40506

S. W. Yates

Department of Chemistry, University of Kentucky, Lexington, Kentucky 40506

(Received 25 March 1985)

Differential elastic and inelastic scattering cross sections have been measured for 2.5 MeV neutrons incident on ^{194}Pt . Scattering to the 0^+ , 2^+ , and 4^+ members of the ground-state band has been measured, as well as to the 2^+ , 3^+ , and 4^+ members of the quasi- γ band. The elastic scattering cross sections have a precision of 2%, and the inelastic scattering cross sections have relative uncertainties ranging from 5% to 15%. The overall normalization uncertainty is 4%. These results, previously measured total cross sections, and very low energy scattering properties are interpreted in a combined analysis which seeks to ascertain the low-lying collective dynamics of ^{194}Pt as made evident in neutron scattering. Coupled-channels calculations employing interacting-boson approximations and pairing-plus-quadrupole nuclear structure models suggest that low-lying excitations of ^{194}Pt are those of a γ -soft nucleus, rather than those of a rigid rotor.

INTRODUCTION

This experiment is part of a program of studies which examines the sensitivity of low energy neutron scattering to several collective excitations of target nuclei, and our ability to determine collective strengths through neutron scattering. Many earlier scattering studies have focused on just a few^{1,2} collective properties of nuclei. The electric quadrupole ($E2$) transition strengths of the first excited 2^+ levels and the octupole ($E3$) strength of the lowest 3^- levels are often well determined in scattering studies. Neutron scattering studies in the incident energy range from about 7 to 11 MeV, for example, have been combined with proton scattering experiments to fix separately target proton and neutron contributions to $E2$ collective excitations of deformed¹ and spherical² nuclei.

Extracting such collective properties with confidence has depended upon combined analyses of elastic and inelastic scattering cross sections and other scattering observables, so that both scattering potentials and target nucleus properties can be confidently determined. Separately determining potential parameters and structure properties of the target nuclei has been a pervasive problem of scattering studies.

Many studies^{3,4} have focused not on target structure, but on the systematic behavior of potential parameters; these works examine parameter dependencies on mass, neutron excess, energy, etc. One result of the systematics oriented studies is that the systematic variations of potential parameters are now fairly well characterized.

At any energy, but particularly at low energies, the advantages of neutron scattering as a probe of structure flow from the fact that one has many observables to constrain parameters in an analysis. These include total cross sections over a wide range of neutron energies, low energy scattering properties such as the s - and p -wave strength functions S_0 and S_1 , and the scattering length R' . Also

included are the differential cross sections for elastic and inelastic scattering. Combining all of this information into an analysis has been systematized⁵ as the SPRT method. S_0 and S_1 constrain potential absorption at low energies in two partial waves, $l=0$ and $l=1$, and R' constrains the refractive properties of the real potential. The total cross sections are fitted from low to intermediate energies, to aid in fixing the energy dependencies of potential parameters. The total cross sections are linear in the scattering amplitudes, which result directly from the choice of potential; they thus provide the most direct test of scattering potentials. Elastic scattering differential cross sections also help constrain the strength of the potential. When all of these properties have been fitted, the scattering potential is rather well determined.⁶

Inelastic scattering cross sections generally contain statistical or compound system (CS) components as well as the direct cross sections which reflect collective strengths. Above 5 MeV incident energy the CS contributions to low-lying excited levels are negligible for medium mass and heavy nuclei,⁶ so that direct coupling analyses account for all of the cross sections. This makes interpretation of cross sections in terms of structure properties direct, and relatively simple. Another useful property is that elastic scattering cross sections show clearly⁶ the presence of strong coupling to scattering from excited levels. However, the elastic scattering cross sections at these higher energies do not differentiate amongst different types of collective excitations;⁶ they are certainly not sensitive to individual matrix elements which couple specific pairs of levels. Inelastic scattering cross sections do show sensitivity to different coupling models, and they are the basis for tests of structure models for incident energies near 5 MeV and above.

The advantages and disadvantages of neutron scattering at lower energies, 2 to 4 MeV, as tests of nuclear structure and dynamics are still being evaluated. A significant ad-

vantage results from the fact that the elastic scattering is much more sensitive to details of different collective models than that at higher energies. A difficulty of low energy analyses arises from the necessity of combining the structure insensitive CS cross sections with the structure sensitive coupled channels components.^{7,8} But rather accurate representations of CS cross sections have been developed, especially during the last ten years, with many encouraging tests of their accuracy.^{9,10} In the case of several strongly excited open channels, different current models of CS components agree with each other to better than 10–15%. Measured cross sections for some excited levels having negligible direct coupled components, for example, unnatural parity states, serve as tests of, and calibrate, the CS cross sections. This issue will be discussed in the Analysis and Interpretation section in the context of the current experiment.

The present program, an extensive set of experiments on the Os and Pt nuclei, was undertaken to test the sensitivity of neutron scattering cross sections to collective properties other than those of the ground-state band. These Os and Pt nuclei were chosen because they are in a shape transitional region, and one in which γ -band excitations are strong and extensively studied.^{11,12} The varying role of these excitations through this mass region is signaled in part by the changing quadrupole moments of the first excited 2^+ levels, so that knowledge of them provides a stringent test of any collective model used in the scattering analyses. It is now clear,¹³ for example, that ^{194}Pt is the nucleus with the quadrupole moment closest to zero of any of the even- A nuclides of this region.

The first of these shape transitional nuclei for which scattering cross sections and analyses are completed is ^{194}Pt . The goal of this first study is to measure precisely and accurately elastic and inelastic scattering cross sections, and then combine these cross sections with information about very low energy scattering properties and total cross sections for determination of both scattering potentials and nuclear structure properties.

EXPERIMENTAL SYSTEM AND METHODS

The experiments were performed at the University of Kentucky 6.5 MV accelerator laboratory using standard pulsed-beam time-of-flight (TOF) methods. Details of the experimental techniques and methods have been published elsewhere.^{3,4,7} A brief description will be presented here. Monoenergetic neutrons were produced via the reaction $^3\text{H}(p,n)^3\text{He}$ in a 3.1 cm long gas cell filled with tritium gas to a pressure of 1 atm. A molybdenum entrance window of approximately 3 mg/cm^2 was used, so that the overall energy spread of neutrons emitted at 0° was 40 keV. The incident proton beam was pulsed and bunched⁷ to a burst width less than 1 ns, with an average current in the ^3H cell of $2\ \mu\text{A}$.

The scattering sample was enriched to 97% in ^{194}Pt , obtained on loan from the Research Materials Collection of the ORNL Isotope Sales Center. Details of the sample composition were given in a companion $(n,n'\gamma)$ study¹⁴ of the structure of ^{194}Pt . The sample was in the form of

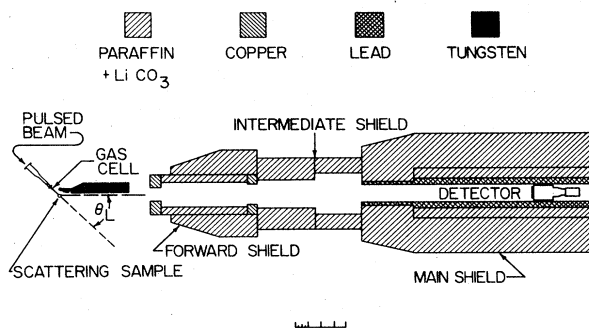


FIG. 1. Scattering geometry with detector collimation. The tungsten shadow bar shields both the scintillation detector at the back of the detector shield and the aperture of the collimator from direct source neutrons.

powdered metal pressed into a polyethylene container 1.5 cm dia by 3 cm height. This 0.2 mole sample was mounted 8.4 cm from the center of the ^3H cell, so that when the effects of the spread of neutron angles is added to the energy spread given above, the average incident neutron energy is 2.5 MeV, with an energy spread whose FWHM is 60 keV. Scattered neutrons were detected in an NE218 liquid scintillator optically coupled to an RCA-8854 photomultiplier. Pulse shape discrimination methods¹⁵ were used to completely eliminate events caused by γ rays in the detector. The scintillator was mounted 2.7 m from the scattering sample in a large shield of Pb, steel, and Li_2CO_3 loaded paraffin. The scattering arrangement is shown in Fig. 1. A typical neutron TOF spectrum obtained in this experiment is shown in Fig. 2. One sees there the key states whose quadrupole excitations were expected to have important influences on the scattering cross sections. The states are the 0^+ , 2^+ , and 4^+ members of the ground state band, and the 2^+ and 4^+ members of the γ band. A small plastic scintillation detector mounted in a polyethylene shield out of the reaction plane was used as an incident flux monitor. It

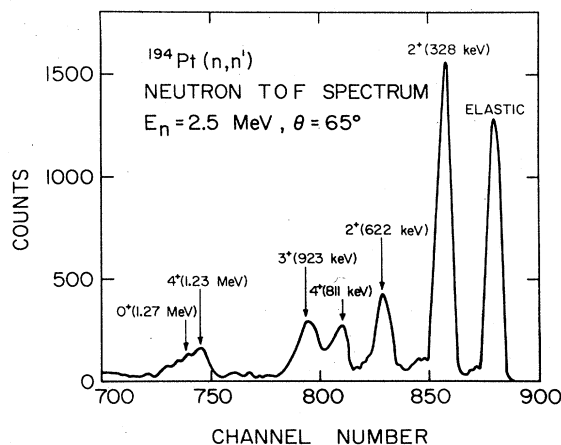


FIG. 2. Time-of-flight spectrum of neutrons scattered from the low-lying levels of ^{194}Pt , showing the collective levels included in the coupled-channels and statistical model analyses reported here.

operated also in a TOF detection mode. A long counter in the reaction plane acted as a secondary monitor, to ensure monitoring stability through redundancy.

The differential scattering yields were normalized to cross sections through use of scattering from carbon, whose scattering cross sections are known well enough to be a secondary standard for neutron scattering.¹⁶ The scattering sample was a 0.5 cm diam by 1.0 cm high cylinder of reactor grade graphite, mounted in place of the ^{194}Pt sample. The rather small sample ensured that sample-size dependent corrections to scattered yields would be small, which results in confident normalization to the known cross sections.¹⁶

The method of using standard normalization cross sections obviates the need to determine neutron flux absolutely, but the energy dependence of the neutron detection efficiency must be well measured. This was accomplished using methods described earlier.¹⁷ Data were accumulated to provide statistical uncertainties of 3% or less for elastic scattering yields and 5% or less for inelastic scattering yields to the 2^+ excited levels. A peak fitting routine developed in our laboratory was used to reproduce the asymmetric peak shapes of the scattering groups, and thus extract yields for the groups of interest in this experiment, labeled in Fig. 2.

RESULTS AND CORRECTIONS

Extracted yields were corrected for electronics dead time, which was never greater than 1%, and for the energy dependence of the neutron detection efficiency. They were also corrected for sample size effects using Monte Carlo methods.¹⁸ These size corrections are for angular

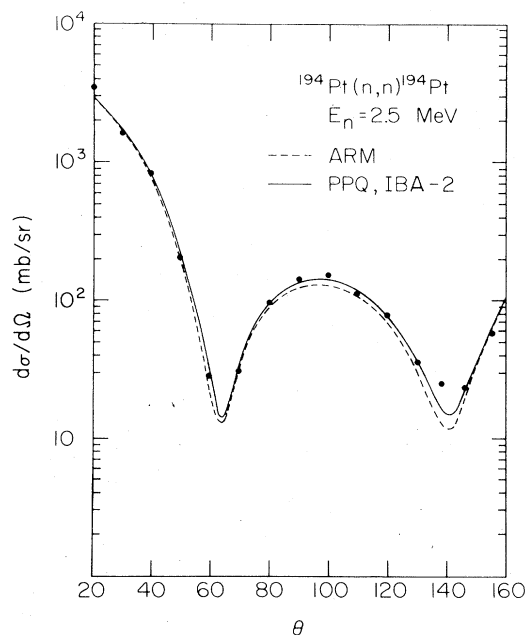


FIG. 3. Measured and calculated elastic scattering differential cross sections. The dashed curve is from the ARM, and the solid curve represents the IBA-1, IBA-2, and PPQ results which are too similar to show separately.

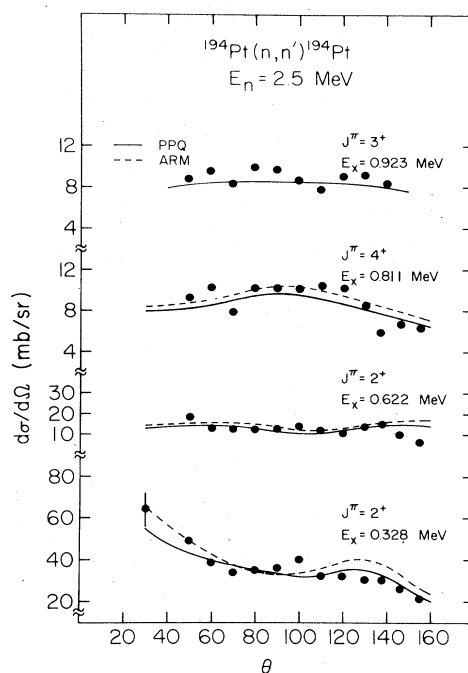


FIG. 4. Measured and calculated cross sections for scattering to excited levels. Curve identifications are those of Fig. 3.

spread of the neutron flux on the sample, flux attenuation, and multiple scattering. The uncertainties associated with the above corrections are contributions to relative uncertainties in that they vary from point to point. They were always less than 5%, and usually 3–4%, for elastic scattering yields. They ranged from 5% to 15% for the inelastic scattering yields, being smallest for the 2^+ levels and largest for the 3^+ level. The overall normalization to the ^{12}C cross sections has an uncertainty of 4%, the systematic uncertainty which is common to all measurements reported here.

The differential elastic scattering cross sections are shown in Fig. 3, and inelastic scattering cross sections are shown in Fig. 4. The various curves shown in those figures are model calculations to be discussed in the next section. Angle-integrated inelastic scattering cross sections are available not only for the levels indicated in Fig. 4, but also for many other levels as well, all from a companion $(n,n'\gamma)$ experiment.¹⁴ From the latter, one obtains γ -ray production cross sections, and then these must be corrected for cascades from high excited levels to lower levels to convert them into inelastic scattering cross sections. The original $(n,n'\gamma)$ yields also must be corrected for sample size effects,¹⁴ similar to the corrections of this experiment, except for γ -ray attenuation replacing the outgoing neutron attenuation. The fully corrected yields from the $(n,n'\gamma)$ experiment are normalized to the present neutron detection results. The ratios of results for the five excited levels separated in both experiments are in excellent agreement, as shown in Table I, a listing of the inelastic scattering cross sections for 16 excited levels of ^{194}Pt . Thus cross sections are included for many levels not resolvable in the present neutron detection experiment.

TABLE I. Measured inelastic scattering cross sections for 16 excited levels of ^{194}Pt . The cross sections for the lowest five excited levels were measured in this experiment and a companion $(n,n'\gamma)$ one. Those for the next ten levels come only from the high resolution γ -ray data. The normalization of the cross sections is that of this neutron scattering experiment.

Excitation energy (keV)	J^π	$\sigma(n,n')$ (mb)	$\sigma(n,n'\gamma)$ (mb)
328.5	2^+	500	478
622	2^+	175	173
811.3	4^+	104	152
922.8	3^+	102	72
1229.6	4^+	65	70
1267.2	0^+		18
1373.9	5^-		95
1411.8	6^+		≤ 7
1422.4	(4^+)		
1432.5	3^-		99
1479.2	0^+		16
1498.7	5^+		19
1511.9	2^+		45
1547.2	0^+		16
1622.2	2^+		33
1670.6	2^+		30

ANALYSIS AND INTERPRETATION

As indicated in the Introduction, the analysis procedure followed was to use low-energy scattering observables and total cross sections to fix the scattering potential for an assumed structure model, and then to test the model by calculating the differential scattering cross sections. Following the SPRT method,⁵ potential parameters were adjusted to reproduce S_0 and R' , and to fit total cross sections over an extended neutron energy range. The measured values¹⁹ of S_0 for natural Pt and for ^{195}Pt are $(1.7 \pm 0.3) \times 10^{-4}$ and $(1.9 \pm 0.4) \times 10^{-4}$, respectively, and the value $R' = (8.7 \pm 0.5)$ fm was measured¹⁹ for ^{194}Pt . Thus in different model tests potential parameters were constrained to give calculated S_0 values in the range $(1.7-1.9) \times 10^{-4}$, as well as fits to the total cross sections. With these constraints, we also obtained $R' \sim 9$ fm. The scattering potential employed was one with a standard geometry, including real, imaginary, and spin-orbit components.^{5,8} The energy dependent potential depths adjusted to fit S_0 and R' values, as well as total cross sections, are shown in Table II.

Total cross sections have been published²⁰ only for natural Pt. Calculated and measured values are shown

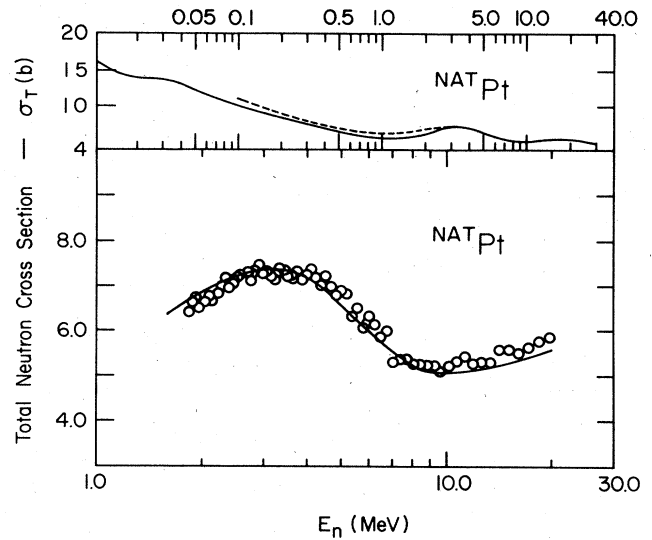


FIG. 5. Total cross sections for natural Pt as a function of neutron energy. The energy scale for the upper panel is at the top of the figure, from 10 keV to 40 MeV, and that for the bottom panel is at the bottom of the figure, from 1.0 to 30.0 MeV. The dashed curve in the top panel is our coupled-channels fit to the data of Ref. 20, represented by the solid curve. The fit is indistinguishable from the data above 3 MeV. Comparisons of that data to new measurements for separated isotopes in this laboratory suggest that the data of Ref. 20 may be several percent low below 3 MeV. Recent data from Ref. 22 are shown as circles in the lower panel, and the solid curve is our coupled channels fit.

over a large energy range in the upper panel of Fig. 5. One sees that the calculations are about 7% high in the lower part of the energy range, but are indistinguishable from the data above 3 MeV. That the energy dependence of the total cross sections at low energies is well represented by the calculations is an important requirement for a realistic model and potential. Recent test measurements²¹ in our laboratory suggest that the data set of the upper panel of Fig. 5 may in fact be 7% low below 1 MeV, where the measurements are most difficult. A new data set, more local in energy, has become available from Poenitz and Whalen.²² Our fit to those total cross sections is shown in the bottom panel of Fig. 5, for a limited energy range which encompasses the incident energy of this experiment. The excellent fit achieved supports the validity of our potential.

The differential scattering cross sections for individual levels arise, at these low energies, from two mechanisms; the first is the CS mechanism in which the cross sections are viewed as composed of independent formation cross

TABLE II. Potential parameters of the real, absorptive, and spin-orbit potentials used to describe ^{194}Pt neutron scattering observables. The notation is that of Refs. 6-8. These potentials provide good fits to all observables when used with the PPQ or IBA-2 models, for measurements from experiments with incident neutron energies below 8 MeV. Potentials and energies are in MeV.

$V = 50.0 - 16[(N-Z)/A] - 0.24E$	$r_R = 1.26$ fm; $a_R = 0.64$ fm
$W_D = 5.30 - 8[(N-Z)/A] + 0.5E$	$r_D = 1.26$ fm; $a_D = 0.47$ fm
$V_{SO} = 5.00$	$r_{SO} = 1.12$ fm; $a_{SO} = 0.47$ fm

sections and decay probabilities in each scattering channel. The original Hauser-Feshbach model has been extensively modified by Moldauer,⁹ to account for level width fluctuations in the compound system and also for the effects of correlations between different scattering channels. In other words, the Hauser-Feshbach model has been modified for an actual lack of independence between formation and decay probabilities. An alternative approach to CS cross sections has been pursued by Weidenmuller and his colleagues over a period of many years. Results of the two approaches were compared by Moldauer and others,^{10,23} and found to be equivalent to within about 10%. The convergence of these two methods provides confidence that the CS cross sections are determined to within about 10–15 %, provided that the scattering potential is well determined.

The CS cross sections calculated depend on the level scheme of ¹⁹⁴Pt. The level schemes in this mass region have been well explored because of the importance of nuclear structures in this shape transitional region. The companion (n,n'γ) study¹⁴ of this nucleus, and references cited therein, provide a detailed level scheme below 2.5 MeV. There are 25 known levels below 2 MeV excitation energy and only a few without definite spin-parity assignments. Level density parameters extracted from systematics and from the known levels below 2.5 MeV permitted us to include the small effects of the large number of unknown levels on the CS cross sections for the known levels. The CS cross sections were first calculated with the large code CINDY (revised),²⁴ designed by Sheldon and Rogers to accommodate calculations for complex level schemes, including the effects of many unobserved levels. A second CS calculation was then done with the code HFCODE developed in this laboratory to include corrections for level width fluctuations and channel-channel correlations in the approximation of Tepel, Hofman, and Weidenmuller.¹⁰ This latter calculation allowed us to ascertain the important compound elastic enhancement,¹⁰ and the corresponding reductions in inelastic CS cross sections, which then are about 10–15 % below values from

the unmodified Hauser-Feshbach model.⁹

The second important mechanism is the direct coupling between incoming and outgoing scattering channels. The coupling is expressed directly in terms of matrix elements⁸ which result from a nuclear structure model, a model to be tested in the experiment. Many of the *E2* matrix elements are also available from measured electric properties, for example, from quadrupole moments and reduced electromagnetic transition probabilities [*B(E2)* values]. Thus a comparison is possible between transition and static moments of an appropriate neutron potential and structure model and those from Coulomb excitation experiments, a comparison which has produced good agreement^{1,8} between neutron scattering and Coulomb excitation for several collective nuclei.

The calculated differential scattering cross sections are then the sum of components from two mechanisms, the structure-insensitive CS and structure-determined direct components. Table III contains a list of *E2* matrix elements calculated from several structure models, whose tests are indicated below. Also listed there are the matrix elements from Coulomb excitation experiments. To maintain the integrity of our model tests, most calculations were performed with a complete model set; that is, individual matrix elements were not altered to correspond to measured values, because that would correspond to a change of model. Tests of each model are then both the comparisons in Table III and comparisons of calculated and measured cross sections.

Coupled channels calculations were done to determine the direct coupling cross sections using the different models of Table III. These and other preliminary model tests were completed using the code²⁵ ECIS-79. In principle, changing the coupling scheme from one model to another would change the effective potential which fits total cross sections and low energy scattering properties, and through the potential changes, the CS cross sections. In practice such potential changes are noticeable only if the model space (number of levels) is changed, or if major changes of collectivity are made. But in the present case

TABLE III. The electric quadrupole transition matrix elements of several nuclear structure models for comparison with the experimental (expt) values. The latter have been extracted from Coulomb excitation and muonic x-ray experiments, Refs. 11, 13, and 27. IBA-1 denotes the IBA model with one set of boson excitation energies and coupling strengths for both neutrons and protons, Refs. 32 and 33. IBA-2 denotes the model using separate excitations for neutrons and protons, Ref. 31. The model PPQ is that of Ref. 34. The reduced matrix elements are normalized to those for excitation of the first 2⁺ level. The parameter κ , in keV, denotes the quadrupole-quadrupole coupling strength in a perturbed IBA-1 model, with notation as in Ref. 12.

J_i	J_f	IBA-1		IBA-2	PPQ	expt
		($\kappa=0.04$)	($\kappa=0.54$)			
0	2	-1.0	-1.0	-1.0	-1.0	-1.0
0	2'	0.0046	0.0627	0.0094	0.053	0.068
2	2	-0.014	-0.196	-0.128	-0.5	-0.13
2	2'	-1.156	-1.142	-1.203	-1.142	±1.14
2	4	1.551	1.552	-1.581	-1.672	±1.58
2'	2'	0.014	0.196	0.026	0.43	0.52
2'	4	-0.0029	-0.0397	-0.223	0.061	-0.03
4	4	-0.0127	-0.175	-0.17	-0.67	0.52

all of the final tests were of models designed to be reasonable for the levels of ^{194}Pt , and thus included the same model space and similar collective strengths. Each model was tested also for reasonable fits to the total cross sections and low energy scattering properties, and only insignificant differences between models were found. Thus the CS cross sections calculated in the manner described above were fixed, and were not varied as different direct coupling models were tested for fits to measured differential scattering cross sections.

As noted, all of the models tested for neutron scattering reflect the well-established^{11,12,27,28} properties of ^{194}Pt . Several studies have produced carefully measured $E2$ strengths for excitation of the first 2^+ level^{11,13,26,27} and all are in good agreement. From these experiments, and with our potential geometry, the value $\beta_2 = -0.16$ is indicated for the quadrupole deformation parameter, reflecting the oblate character of this nucleus (and of other stable Pt nuclei). Determinations of the hexadecapole moment^{11,27} show that $\beta_4 = -0.04$. Since these are now well-determined strengths of this nucleus, they were held fixed throughout our coupled channels tests.

The well documented and important nonaxial quadrupole excitations of Pt nuclei^{11,13,27} make it clear that all realistic models must include the γ -band excitations. The first realistic model test, then, is that of the rigid asymmetric rotor (ARM), or Davydov-Filippov, model,²⁸ which provides $E2$ moments dependent on both β_2 and on the asymmetry parameter, γ . The degree of nonaxiality of the quadrupole excitations of ^{194}Pt is determined by that asymmetry parameter. For the even- A Pt nuclei the low excitation energies of the second 2^+ levels and $E2$ transition strengths from 2^+ levels requires near maximum departure from axial symmetry. Originally, then, the parameter γ was determined from 2^+ excitation energies.²⁸ However, it is apparent that minor mixing between the first and second 2^+ levels and other 2^+ levels can alter energy positions of them, without altering excitation intensities significantly. Since it is these intensities that are really being tested in transition rate analyses, we determine γ from the $B(E2)$ for the 0^+ to 2^+ transition and from the quadrupole moment for the latter level. In this way, we determine $\gamma = 31.1^\circ$, a result consistent both with γ -band energy spacings and transition rates. Calculations with this model are shown in Figs. 3 and 4 as dashed curves, for elastic and inelastic scattering, respectively. The fit to the elastic scattering is poor. We define a goodness of fit criterion, Q^2 , which is the uncertainty weighted sum of squares of deviations of calculated from measured cross sections:

$$Q^2 = \sum_i (\sigma_{\text{calc}}^i - \sigma_{\text{exp}}^i)^2 / (\Delta\sigma)^2,$$

where σ_{calc} and σ_{exp} are the calculated and experimental cross sections, respectively, and $\Delta\sigma$ is the experimental uncertainty. The sum is over all angles of measurement of differential cross sections. This Q^2 is 2.5 times worse for the dashed curves of both Figs. 3 and 4 than the Q^2 for the solid curves, to be discussed below, and the curves are well outside the uncertainties of the measurements. The points plotted in Fig. 3 are actually larger than the

uncertainties of those measurements. The high Q^2 for the inelastic scattering cross sections of Fig. 4 results from the poor fit of the ARM to the data for the first 2^+ level for angles beyond 100° . Perhaps the most serious discrepancy is that for elastic scattering, because these are the most precise data. Changes in potentials could be made to remove most of the discrepancy, but then the low energy scattering properties and total cross sections would not be fit. Baker *et al.*²⁹ also noted the failure of the ARM calculations to fit their 78 MeV ^{12}C scattering data for ^{194}Pt ; but they had not included $E4$ excitation of the 4^+ level, as was done here for the ARM calculations shown in Figs. 3 and 4. They then extended their ARM to include $E4$ excitations, and also found it necessary to change the parameter γ to 42° . With this altered ARM, they did obtain good fits to the ^{12}C scattering data. Yadav *et al.*³⁰ point out, however, that this large γ value is inconsistent with the level spacings of the γ band. We note it is also inconsistent with the $E2$ moments associated with the first 2^+ level. Thus neither the ^{12}C scattering data nor our neutron scattering data can be well described with an ARM which is consistent with the bound level structure of ^{194}Pt .

Several recent structure models, whose geometric character is rather different than that of the ARM, have been used to describe the levels and electromagnetic transitions in ^{194}Pt . The most extensively calculated of these models are the interacting boson approximations (IBA). The first is one which uses one set of boson excitation energy and residual coupling for both protons and neutrons (IBA-1),¹² and the second is another which provides a more detailed fit to energies and electromagnetic transition rates, at the expense of additional complexity by invoking separate boson excitations³¹ for neutrons and protons (IBA-2).

The IBA-1 calculations are based on models of nuclei in the Os-Pt region by Casten and Cizewski.¹² These authors show nuclei of this mass region as representing smoothly developing departures from the O(6) symmetries, represented best by ^{196}Pt . Deason³² used the ^{194}Pt parameters of Ref. 12 to calculate the matrix elements shown in the third column of Table III. In an important study of scattering from Pt nuclei Deason *et al.*³³ found the best description of 35 MeV proton scattering from ^{194}Pt to correspond to a small modification of the perturbed O(6) symmetry proposed in Ref. 12. The $E2$ matrix elements from that modification are in the fourth column of Table III. The most important difference for scattering in the two IBA-1 models is in the 0^+ to 2^+ matrix elements. But at our low neutron energy we cannot differentiate between those small values. Both $E2$ and $E4$ matrix elements for the IBA-1 models were kindly provided to us by Ronningen and Deason.³² The $E2$ matrix elements for the levels included in our analyses are listed in Table III for two different coupling strengths between s and d bosons, using the notation of Casten and Cizewski.¹² The cross sections calculated here were done in a model space of six levels, the $J=0, 2$, and 4 levels of the ground state band and the $J=2, 3$, and 4 levels of the γ band. Much of the preliminary testing could be done with a smaller model space, dropping the 3^+ and second 4^+ levels. The direct coupling cross sections to those two

levels at our incident energy were only a few percent of the measured cross sections, and they had negligible effect on the calculations for other levels.

Cross sections calculated with the two sets of IBA-1 matrix elements gave results negligibly different from each other. A full, six level calculation gives results for elastic scattering close to the solid curve of Fig. 3. The fit to the elastic scattering is thus acceptable, although the Q^2 is 50% worse than that for the best calculations. The IBA-1 fits to the inelastic scattering cross sections of Fig. 4 are good, except the fit to the first excited 2^+ level forward of 60° . At small angles that calculation is two standard deviations below the measurements, suggesting that the IBA-1 model, while much better than the ARM, still does not describe all of the data. It provides an adequate fit for the elastic scattering cross sections, but fails to reproduce the forward peaking observed for the first excited 2^+ level. That failure is associated with the sign of the large 2^+ to 4^+ matrix element. The IBA-1 2^+ calculation is not shown.

The two most successful models are the pairing-plus-quadrupole (PPQ) model of Kumar,³⁴ and the IBA-2 model of Bijker *et al.*,³¹ which provide quite similar large $E2$ matrix elements, as is seen in Table III, and indistinguishable fits to the cross sections. A six level coupled channels calculation with the PPQ reduced matrix elements where they are available, and using the IBA-2 values for the few not provided in Ref. 34, is shown as the solid curves of Figs. 3 and 4. These two models provide calculated cross sections with the smallest Q^2 for the fit for all levels together, and the best fit separately to the elastic scattering cross sections and to the inelastic scattering cross sections to the first 2^+ level. The quality of the fit is consistent with the accuracy of the measurements.

SUMMARY AND CONCLUSIONS

This experiment was begun in the expectation that at low incident neutron energies scattering cross sections would show a substantial sensitivity to quadrupole excitations of the γ band, just as previous experiments had shown great sensitivity to ground state band excitations.⁶⁻⁸ We suspected that the elastic scattering cross sections at low incident neutron energy would be sufficiently sensitive to nonaxial or γ band excitations that information about the strength and character of those excitations could be extracted from them, in spite of the fact that γ -band excitation strengths are a factor of 5 weaker than the excitation strength of the first 2^+ level. The present experiment and analysis confirms that the combination of elastic and inelastic scattering cross sections provides sufficient sensitivity to discriminate between γ -soft models and γ -rigid ones, such as the ARM. The differences between different dynamical models is not large, however. Testing them requires accurate, high confidence measured cross sections and careful attention to

details of the determination of the scattering potential. Without the availability of low-energy scattering properties and total cross sections to constrain the scattering potential, the tests offered here would be impossible. It is the requirement of a consistent treatment of all of the information that makes model discrimination possible.

There are two points to be made about the confidence with which conclusions can be drawn from this experiment and analysis. First, statistical or compound system models have been developed to the point that CS cross sections can be calculated with model uncertainties no larger than about 10–15%. This conclusion is particularly strong when one examines cross sections for strongly excited channels, and when many scattering channels are open.²³ But the CS cross sections can be regarded with such confidence only if the scattering potential is carefully determined to be appropriate for the nucleus studied. In this study the CS mechanism accounts for 98% of the cross section to the 3^+ level; the agreement between calculation and measurement supports the validity of the potential determined. The second point is associated with the very small value of the $E2$ moment for direct excitation of the second 2^+ level, as listed in Table III. Models which provide small but different values for that matrix element cannot be differentiated in this study, because the CS component dominates the second 2^+ cross section.

The three models indicated in Table III, IBA-1, PPQ, and IBA-2, all describe the low-lying levels and decay schemes of ^{194}Pt . Deason *et al.*³³ had found that the IBA-1 matrix elements of Table III provided a good fit to their 35 MeV proton scattering data; our results show a preference for the IBA-2 and PPQ models. It would be quite useful to test the IBA-2 and PPQ models for proton scattering with a potential designed to be consistent with that determined here for neutron scattering. Such calculations are now in progress.

The best tentative suggestion for the collective behavior of ^{194}Pt can be drawn from the two IBA models and the PPQ model. They imply a γ -soft vibrational nucleus without well-defined shape at low excitation energies. These interpretations need to be confirmed through neutron scattering measurements at higher energies and a combined analysis of proton, neutron, and ^{12}C scattering in a common model context. The measurements and analyses are in progress.

ACKNOWLEDGMENTS

The authors are grateful to P. T. Deason and R. M. Ronningen who provided us with a copy of Deason's dissertation and detailed information about IBA matrix elements. We are also indebted to R. Bijker who provided us with detailed tabulations of the IBA-2 matrix elements used in the analyses reported here. This work was supported through a grant from the National Science Foundation.

- *Permanent address: Physics Department, Yarmouk University, Irbid, Jordan.
- †Permanent address: Service de Physique Nucleaire et Neutronique, Centre d'Etudes de Bruyères-le-Châtel, 91680 France.
- ¹Ch. Lagrange, J. Lachkar, G. Haouat, R. E. Shamu, and M. T. McEllistrem, Nucl. Phys. **A345**, 193 (1980).
 - ²R. W. Finlay, J. Rapaport, M. H. Hadizadeh, M. Mirzaa, and D. E. Bainum, Nucl. Phys. **A388**, 45 (1980).
 - ³M. T. McEllistrem, in Proceedings of the Conference on Interactions of Neutrons with Nuclei, edited by E. Sheldon, ERDA Report, CONF-760715-P1, 1976.
 - ⁴J. L. Weil, Proceedings of the Conference on Scientific and Industrial Applications of Small Accelerators, IEEE Trans. Nucl. Science **NS-28**, 1255 (1981).
 - ⁵J. P. Delaroche, Ch. Lagrange, and J. Salvy, in *Nuclear Theory in Neutron Nuclear Data Evaluation* (IAEA, Vienna, 1976).
 - ⁶M. T. McEllistrem, R. E. Shamu, J. Lachkar, G. Haouat, Ch. Lagrange, Y. Patin, J. Sigaud, and F. Cocu, Phys. Rev. C **15**, 1927 (1977); J. Lachkar, Proceedings of the Conference on Neutron Physics and Nuclear Data for Reactors and Other Applications, Harwell, England, 1978.
 - ⁷D. F. Coope, M. C. Schell, S. N. Tripathi, and M. T. McEllistrem, Phys. Rev. Lett. **37**, 1126 (1976); D. F. Coope, S. N. Tripathi, M. C. Schell, J. L. Weil, and M. T. McEllistrem, Phys. Rev. C **16**, 2223 (1977).
 - ⁸J. P. Delaroche, G. Haouat, J. Lachkar, Y. Patin, J. Sigaud, and J. Chardine, Phys. Rev. C **23**, 136 (1981); J. P. Delaroche, *ibid.* **26**, 1899 (1982).
 - ⁹P. A. Moldauer, Phys. Rev. C **11**, 426 (1975); **12**, 744 (1975); **14**, 764 (1976).
 - ¹⁰J. W. Tepel, H. M. Hofman, and H. A. Weidenmuller, Phys. Lett. **49B**, 1 (1974).
 - ¹¹C. Baktash, J. X. Saladin, J. J. O'Brien, and J. G. Alessi, Phys. Rev. C **18**, 131 (1978).
 - ¹²R. F. Casten and J. A. Cizewski, Nucl. Phys. **A309**, 477 (1978).
 - ¹³C. Y. Chen, J. X. Saladin, and Abdul A. Hussein, Phys. Rev. C **28**, 1570 (1983); M. V. Hoehn, E. B. Shera, H. D. Wohlfahrt, Y. Yamazaki, and R. M. Steffen, Bull. Am. Phys. Soc. **24**, 53 (1979).
 - ¹⁴A. J. Filo, S. W. Yates, D. F. Coope, J. L. Weil, and M. T. McEllistrem, Phys. Rev. C **23**, 1938 (1981).
 - ¹⁵D. W. Glasgow, D. E. Velkley, J. D. Brandenberger, and M. T. McEllistrem, Nucl. Instrum. Methods **114**, 535 (1974).
 - ¹⁶A. Smith, R. Holt, and J. Whalen, Argonne National Laboratory Report ANL/NDM-43, 1978 (unpublished); R. Schwartz, R. Schrack, and D. Heaton, National Bureau of Standards Publication NBS-138, 1974.
 - ¹⁷F. D. McDaniels, J. D. Brandenberger, G. P. Glasgow, and H. G. Leighton, Phys. Rev. C **10**, 1987 (1974), and references cited therein.
 - ¹⁸D. E. Velkley, D. W. Glasgow, J. D. Brandenberger, and M. T. McEllistrem, Nucl. Instrum. Methods **129**, 231 (1975).
 - ¹⁹S. F. Mughabghab and D. I. Garber, Brookhaven National Laboratory Report BNL-325, 1973.
 - ²⁰D. I. Garber and R. R. Kinsey, Brookhaven National Laboratory Report BNL-325, third edition, 1976, Vol. II.
 - ²¹S. E. Hicks, Z. Cao, J. Hanly, and M. T. McEllistrem, Bull. Am. Phys. Soc. **28**, 984 (1983).
 - ²²W. P. Poenitz and J. F. Whalen, Argonne National Laboratory Report ANL/NDM-80, 1983.
 - ²³P. A. Moldauer, in Proceedings of the Conference on Interactions of Neutrons with Nuclei, edited by E. Sheldon, ERDA Report, CONF-760715, 1976, p. 243; J. W. Tepel, H. M. Hofman, and M. Herman, Proceedings of the International Conference on Nuclear Cross Sections for Technology, Nat. Bur. Stand. (U.S.) Special Publ. **594**, 762 (1980); P. A. Moldauer, Bull. Am. Phys. Soc. **28**, 688 (1983).
 - ²⁴E. Sheldon and V. C. Rogers, Comput. Phys. Commun. **6**, 99 (1973); and E. Sheldon, private communication.
 - ²⁵J. Raynal, ECIS79 (unpublished); J. Raynal, *Computing as a Language of Physics* (IAEA, Vienna, 1972); *The Structure of Nuclei* (IAEA, Vienna, 1972), p. 75.
 - ²⁶I. Y. Lee, D. Cline, P. A. Butler, R. M. Diamond, J. O. Newton, R. S. Simon, and F. S. Stephens, Phys. Rev. Lett. **39**, 684 (1977).
 - ²⁷C. Y. Wu, D. Cline, A. Backlin, B. Kotlinski, and C. Baktash, Bull. Am. Phys. Soc. **28**, 687 (1983).
 - ²⁸A. S. Davydov and G. F. Filippov, Nucl. Phys. **8**, 237 (1958).
 - ²⁹F. T. Baker, A. Scott, T. P. Cleary, J. L. C. Ford, E. E. Gross, and D. C. Hensley, Nucl. Phys. **A321**, 222 (1979); F. T. Baker, *ibid.* **A331**, 39 (1979).
 - ³⁰H. L. Yadav, B. Castel, and H. Toki, Phys. Rev. C **22**, 2644 (1980).
 - ³¹R. Bijker, A. E. L. Dieperink, O. Scholten, and R. E. Spanhoff, Nucl. Phys. **A344**, 207 (1980).
 - ³²P. T. Deason, Jr., Ph.D. dissertation, Michigan State University, 1979 (unpublished); and R. M. Ronningen, private communication.
 - ³³P. T. Deason, C. H. King, R. M. Ronningen, T. L. Khoo, F. M. Bernthal, and J. A. Nolen, Phys. Rev. C **23**, 1414 (1981).
 - ³⁴K. Kumar, Phys. Lett. **29B**, 25 (1969).